ELSEVIER

Journal of Alloys and Compounds 323–324 (2001) 223–230

Journal of ALLOYS AND COMPOUNDS

www.elsevier.com/locate/jallcom

Rare earth fluorosulfides LnSF and $Ln_2AF_4S_2$ as new colour pigments

A. Demourgues[a,b,*], A. Tressaud[a], H. Laronze[a], P. Macaudière[b]

[a] *ICMCB-CNRS, 87 Avenue du Dr A. Schweitzer, 33608 Pessac, Cedex, France*
[b] *RHODIA, CRA, 52 rue de la Haie Coq, 93308 Aubervilliers, Cedex, France*

Abstract

Rare earth fluorosulfides LnSF and $Ln_2AF_4S_2$ (A=Ca, Sr) have been prepared and characterized by X-ray diffraction. The structures can be described as the succession of various sheets of rare earth or alkaline earth, fluorine and sulfur. Thus in these compounds, rare earth is at the center of a distorted square antiprism with four F atoms on one base, four S in the other and a fifth Ln–S bond parallel to the *c* axis. These compounds exhibit interesting colour from yellow (Sm, Gd) to red (Ce). The chromatic properties have been correlated to structural features and mechanisms at the origin of the colour have been proposed. The variation of energy of absorption edge as a function of rare earth has been explain in terms of ionization energies.

Keywords: Colour pigments; Fluorosulfides; Structure determination; Diffuse reflectance; Electronic transitions

1. Introduction

The chromatic properties of rare earth sesquisulfides Ln_2S_3 and ALn_2S_4 (A=Ca, Sr) have been recently investigated: these compounds exhibit pronounced colour ranging from yellow to red which depends on the rare earth [1,2]. The colour of these compounds has been related to various energetic parameters such as ionization energies, crystal field splitting or nephelauxetic effect, the positions of energetic levels in the valence and conduction bands being a function of the crystal structure. These sulfides adopt the γ-Th_3P_4 type structure (cubic *I43d*) where the rare earth is eight-fold coordinated to sulfur in a triangulated dodecahedral site [2,3]. However these compounds are unstable in acidic medium and some applications become therefore tricky. Most of fluorides and mixed-anion compounds containing fluorine exhibit good stability in this medium due to the small size and high electronegativity of fluorine atom and its tendency to generate acidity. Rare earth fluorosulfides LnSF (Ln=La, Ce, Pr, Nd, Sm, Gd) have been prepared and characterized by X-ray diffraction (XRD). LnSF compounds which adopt the PbFCl type structure had been investigated few years ago [4,5] but the results were still questionable [5,6]. In these compounds, the environment of rare earth, which is surrounded by both fluorine and sulfur atoms, is different from that in rare earth sesquisulfides [7]. New methods of synthesis of LnSF have been recently proposed [8]. A reinvestigation of these compounds by XRD and EXAFS has been thus carried out in order to get accurate informations about the rare earth environment. Moreover, new compounds with $ALn_2F_4S_2$ (A=Ca, Sr) formulation have been prepared and characterized by XRD. The diffuse reflectance spectra have been measured and the colour of these compounds has been discussed in terms of ionization energies of rare earth, crystal field and nephelauxetic effect related to the environment of rare earth.

2. Experimental

2.1. Preparation of materials

Rare earth fluorosulfides LnSF and $Ln_2AF_4S_2$ (A=Ca, Sr) were synthesized by reaction of stoichiometric quantities of high purity rare earth sulfides Ln_2S_3 in their α form, rare earth fluorides and alkaline-earth fluorides (LnF_3 and AF_2). Fluorides were purified under F_2 or HF at temperatures varying from 500 to 800°C. α-Ln_2S_3 sulfides were prepared starting from reaction involving pure rare earth metal and sulfur, slowly heated on sealed quartz tubes at 400°C for 24 h and at 700°C for 24 h. These compounds were mixed in a glove box and the mixture was placed in a carbon crucible inside a sealed quartz tube. For polycrystalline samples in the case of LnSF, the mixture of stoichiometric amount of rare earth fluoride and

*Corresponding author. Fax: +33-556-842-761.
E-mail address: demourg@icmcb.u-bordeaux.fr (A. Demourgues).

0925-8388/01/$ – see front matter
PII: S0925-8388(01)01116-1

rare earth sulfide is annealed up to 900°C. In the case of polycrystalline $Ln_2AF_4S_2$, this temperature is equal to 1100°C. In order to obtain single crystals of $Ln_2AF_4S_2$, the mixture is slowly heated up to 1200°C (15°C/h) and slowly cooled down to room temperature (5°C/h).

2.2. X-ray diffraction and absorption experiments

Powder XRD (Philips PW 1050, CuKα radiation) indicated that all samples crystallized with tetragonal symmetry (space group: *P4/nmm*, No. 129). The Rietveld method were used for refinement of powder XRD data using a pseudo-Voigt profile function. Integrated intensities, position and structural parameters were refined in 10–120°(2θ) range with integration times of 40 s using the FULLPROF program package [9]. For $Ln_2AF_4S_2$ composition, single crystals were obtained. Intensity data were collected on an ENRAF Nonius CAD4 form circle diffractometer using graphite monochromated MoKα radiation. Intensity treatment and refinement calculations were performed using the SHELXL93 program [10]. EXAFS spectra at the Ce L_{III}-edge were collected on station 7.1 at the Daresbury synchroton radiation source, in transmission mode using a Si (111) monochromator crystal. Ce L_{III} edge were reduced to normalized XAFS $\chi(k)$ using Daresbury software, and weighted $k^3\chi(k)$ data were analyzed using the EXCURV suite of programs [11]. Diffuse reflectance spectra were recorded on a Cary 17 spectrophotometer in the visible region.

3. Results and discussion

3.1. X-ray diffraction study

The LnSF phases (Ln = La, Ce, Pr, Nd, Sm, Gd) adopt a tetragonal symmetry with the *P4/nmm* space group related to the PbFCl type-structure. The *a* and *c* parameters decrease continuously as a function of rare earth ionic size (Table 1). Solid solutions $Ln_{0.66}Ln'_{0.33}SF$ have been prepared and the corresponding *a* and *c* parameters fit well into the LnSF series. The rare earth and sulfur atoms occupy the *2c* sites whereas the fluorine atoms are placed in the *2a* site. The powder X-ray diffractograms of LnSF phases have been refined by the Rietveld method in order to determine accurately the atomic positions. The atomic positions, isotropic thermal displacement and reliability factors (R_B, R_P, R_{wp}) of GdSF are given in Table 2. These results are in good agreement with those of CeSF and SmSF [8] and differ from previous results obtained by Batsanov et al. [6] and Dagron et al. [5]. In order to confirm the atomic positions determined by Rietveld refinement of powder X-ray diffractograms, EXAFS experiments were undertaken on CeSF at the Ce L_{III} edge. Good quality spectra were obtained up to $k = 11$ Å^{-1} (Fig. 1). The Ce–S, Ce–F and Ce–Ce radial distance and the Debye–Waller factors associated have been determined and the results are reported in Table 3a. Finally four Ce–F distances at 2.56 Å and five Ce–S distances at 2.92 Å have been refined. These results are in good agreement with those obtained from XRD data refinement (Table 3b). The four Ln–F distances decrease from 2.58 Å (La) to 2.48 Å (Gd). As far as the Ln–S bond distances are concerned, two groups of four Ln–S bond lengths and one Ln–S distance that corresponds to the apical sulfur atom, have been identified. The four Ln–S bond length decrease rapidly from 2.98 Å (La) to 2.84 Å (Gd) whereas in the case of the unique Ln–S bond distance, the amplitude of variation becomes smaller (from 2.91 Å (La) to 2.85 Å (Gd)). Thus, in the case of Sm and Gd, the five Ln–S bond distances are almost equal. The bond distances are reported in Table 4. In the $Na_{0.5}Ln_{2.5}S_4$ or $SrLn_2S_4$ sesquisulfides, which adopt the γ-Th_3P_4 type structure, the rare earth is surrounded by four sulfur atoms at 2.83–2.97 Å ($SrCe_2S_4$: 2.93 Å) and four other ones at 3.0–3.15 Å ($SrCe_2S_4$: 3.1 Å) [3]. The Ln–S distances found in LnSF are comparable to the smaller Ln–S bond lengths found in rare earth sesquisulfides. Finally the comparison of EXAFS and XRD results and the evolution of Ln–S and Ln–F bond lengths lead to reject definitively previous data on LnSF phases, in which lower unit cell parameters, shorter Ln–F bond lengths and larger Ln–S distances were indeed mentioned.

In LnSF, the environment of rare earth, surrounded by 4 fluorine atoms and (4+1) sulfur atoms, differs from that in sesquisulfides ALn_2S_4 where the rare earth occupy a triangulated dodecahedral site (two tetrahedral sites, 4+4

Table 1
Unit-cell constants of LnSF (La–Gd)

Compounds	Cell parameters (Å)
LaSF	$a = 4.0398(3)$
	$c = 6.9697(6)$
CeSF	$a = 3.9917(2)$
	$c = 6.9473(6)$
PrSF	$a = 3.9569(2)$
	$c = 6.9226(5)$
NdSF	$a = 3.9278(1)$
	$c = 6.9056(2)$
SmSF	$a = 3.8723(2)$
	$c = 6.8755(4)$
GdSF	$a = 3.8297(1)$
	$c = 6.8529(2)$

Table 2
Atomic positions, isotropic thermal displacements and reliability factors of GdSF

GdSF $R_B = 2.9\%$, $R_p = 9.8\%$, $R_{wp} = 4.7\%$					
Atoms	Site	*x*	*y*	*z*	B_{eq} (Å^2)
Gd	*2c*	1/4	1/4	0.2295(2)	0.39(3)
S	*2c*	1/4	1/4	0.6450(6)	0.4(1)
F	*2a*	3/4	1/4	0	0.7(3)

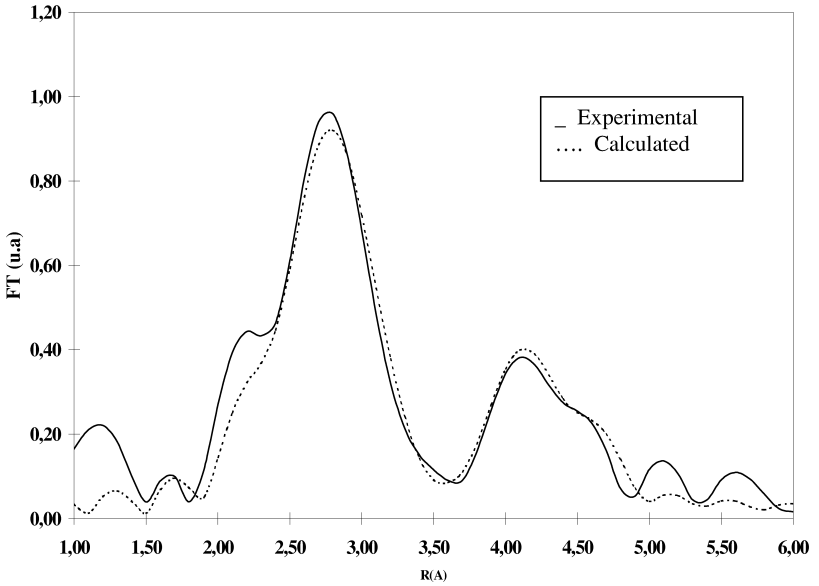

Fig. 1. Fourier transform of experimental and calculated XAFS spectra of CeSF at Ce L_{III} edge.

Table 3
Interatomic distances in CeSF taken from XAFS analysis and Rietveld refinement

Analysis	Interatomic distances					
	Ln–F (Å)	σ^2 (Å^2)	Ln–S (Å)	σ^2 (Å^2)	Ln–Ln (Å)	σ^2 (Å^2)
EXAFS	2.56×4	0.017	2.92×5	0.012	3.97×4	0.013
			4.02×1	0.012	4.27×4	0.021
XRD	2.564(2)×4		2.91(2)×1		3.992(1)×4	
			2.940(3)×4		4.280(3)×4	
			4.04(1)×1			

neighbors). The sesquisulfides adopt a 3D type-structure, the crystal structure of LnSF phase has a 2D character.

The rare earth is at the center of a distorted square antiprism with four F atoms in one base and four S atoms in the other, as shown in Fig. 2. A fifth Ln–S bond smaller than the other ones appears parallel to the *c* axis. The structure can be described as a succession of various sheets of rare earth, fluorine and sulfur, the sequence being [S–Ln–F–Ln–S][S–Ln–F–Ln–S]. In this sequence, two layers or blocks can be identified: the $[Ln_2F_2]^{4+}$ fluorite-like layers which alternate with double $[S_2]^{4-}$ layers along the *c* axis. In order to modify the structure of fluorite-like

Table 4
Coordination polyhedra of rare earths in LnSF

Compounds	Ln–S (Å) distances	Ln–F (Å) distances
LaSF	2.980(5)×4	2.581(2)×4
	2.91(2)×1	
CeSF	2.940(3)×4	2.564(2)×4
	2.91(2)×1	
PrSF	2.920(4)×4	2.544(2)×4
	2.89(2)×1	
NdSF	2.902(2)×4	2.527(1)×4
	2.883(9)×1	
SmSF	2.87(2)×1	2.498(2)×4
	2.867(4)×4	
GdSF	2.848(6)×1	2.478(2)×4
	2.841(2)×4	

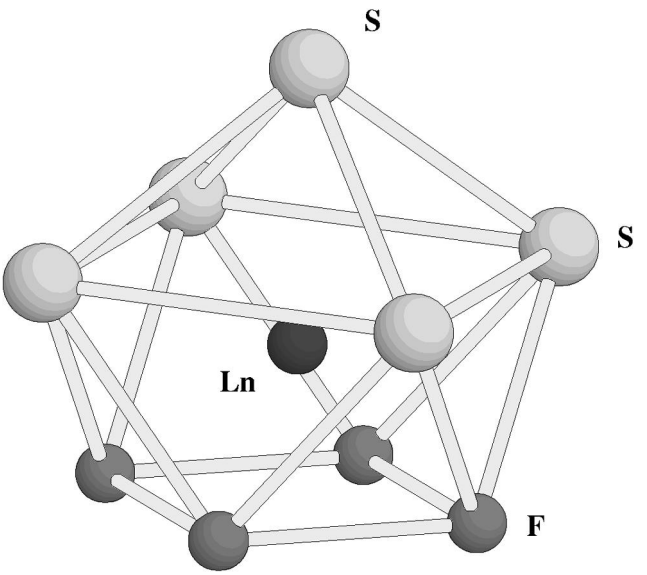

Fig. 2. Environment of Ln in LnSF.

Table 5
Atomic positions and isotropic thermal displacements of $Sm_2CaF_4S_2$ (single crystal analysis) and $Ce_2SrF_4S_2$ (powder Rietveld analysis) compounds

Atoms	Site	x	y	z	U_{iso} (Å^2)	Occupancies
$Sm_2CaF_4S_2$ ($I4/mmm$)				$R_{int}=5.48\%$	$R_I=1.51\%$	$wR=3.31\%$
$a=3.91594(5)$ Å, $c=19.2530(5)$ Å						
Sm1	*4e*	0	0	0.15651(1)	0.0076(3)	0.84
Ca1	*4e*	0	0	0.15651(1)	0.0076(3)	0.16
Sm2	*2b*	0	0	1/2	0.0082(4)	0.32
Ca2	*2b*	0	0	1/2	0.0082(4)	0.68
S	*4e*	1/2	1/2	0.19377(6)	0.0089(3)	1
F	*16n*	0	0.397(1)	0.0659(2)	0.0186(6)	0.5
$Ce_2SrF_4S_2$ ($I4/mmm$)				$R_B=7\%$	$R_p=15.1\%$	$R_{wp}=17.9\%$
$a=4.0782(2)$ Å, $c=19.637$ (1) Å						
					B_{eq} (Å^2)	
Ce1	*4e*	0	0	0.1586(3)	0.5(2)	0.80
Sr1	*4e*	0	0	0.1586(3)	0.5(2)	0.20
Ce2	*2b*	0	0	1/2	0.6(2)	0.39
Sr2	*2b*	0	0	1/2	0.6(2)	0.61
S	*4e*	1/2	1/2	0.1888(8)	1.3(4)	1
F	*16n*	0	0.384(8)	0.064(2)	1.4(9)	0.5

layers and consequently the environment of rare earth related to the color of these compounds, we have investigated the Ln_2S_3–AF_2 (A=Ca, Sr) systems in order to identify new colored pigments. New phases $Ln_2AF_4S_2$ crystallizing in a tetragonal mode (Bravais mode: I) have been found. The *a* parameter is close to that of LnSF whereas the *c* parameter is equal to a(AF_2)+2c(LnSF), i.e. around 19 Å. The structure has been firstly determined from a single-crystal of $Sm_2CaF_4S_2$ and has been solved in the $I4/mmm$ (No. 139) space group (Weissenberg and precession photographs) ($R_{int}=5.48\%$, $R_I=1.51\%$, $wR=3.31\%$, Table 5). All the $Ln_2AF_4S_2$ phases (Ln=La–Gd, A=Ca, Sr) adopt the same structure. In the case of $Ce_2SrF_4S_2$ phase, the powder XRD pattern has been refined by the Rietveld method ($R_B=7\%$, $R_P=15.1\%$, $R_{wp}=17.9\%$) (Fig. 3). The *R* values are relatively high because of the presence of small amount (5%) of $SrCe_2S_4$ impurity. Heavy elements such as Ce and Sr are statistically distributed in 4*e* (0,0,*z*) and *2b* (0,0,1/2) positions (Table 5), the occupancy of Ce being 0.8 in the *4e* site and 0.4 in the *2b* site. Thus, the following formula can be written: $[Ce_{1.6}Sr_{0.4}]$(4e) $[Ce_{0.4}Sr_{0.6}]$(2b) F_4S_2. Another *4e*

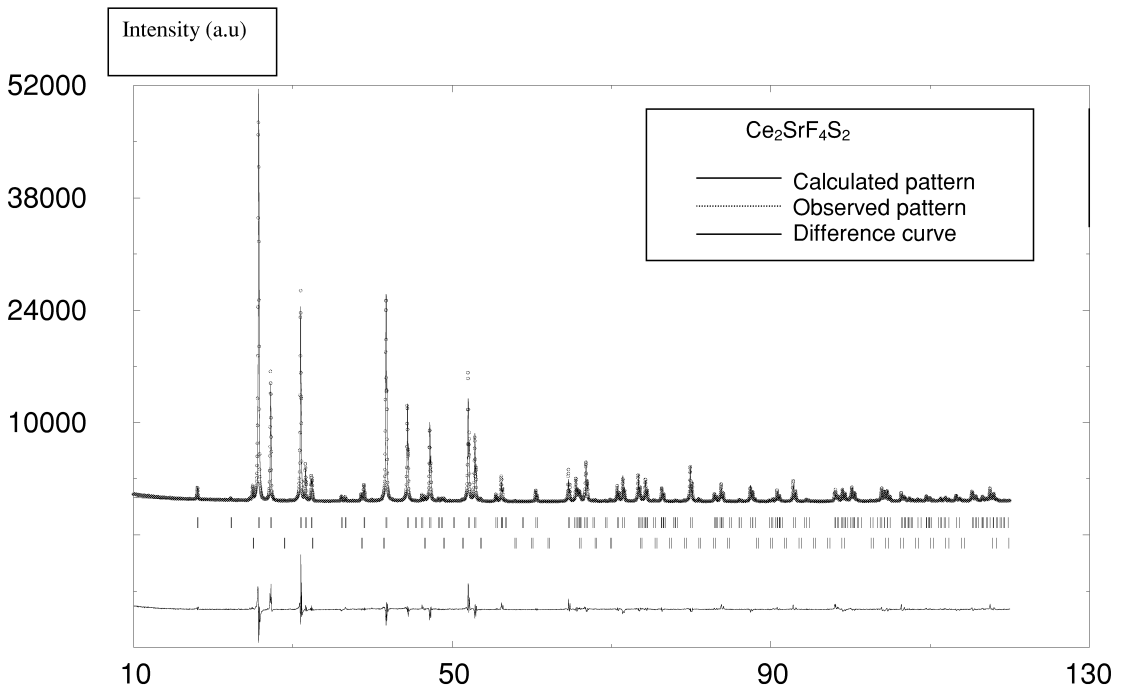

Fig. 3. Observed (dots), calculated (full line) XRD patterns and difference curve of $Ce_2SrF_4S_2$ (2θ, CuKα).

site is fully occupied by S atoms. However, fluorine atoms occupy partially the *16n* position (0,$y \approx 0.40$,z), the occupancy being equal to 0.5. The *8g* position (0,1/2,z), close to the previous *16n* ones, is not suitable because the isotropic thermal displacement is too high for this site.

The structure of $Ce_2SrF_4S_2$ is presented in Fig. 4. The $[Ln_2F_2]^{4+}$ layers in LnSF are replaced in $Ln_2AF_4S_2$ by larger and more complex sheets with $[Ln_2AF_4]^{4+}$ formula. These sheets (Fig. 4) are always separated by double layers of sulfur atoms with $[S_2^{4-}]$ formula. In $Ln_2AF_4S_2$, the A(Ln) (*2b* site) is 8-fold coordinated to fluorine while Ln(A) (*4e* site) is 4-fold coordinated to fluorine and 8-fold coordinated to sulfur as in LnSF. The Ce(Sr)–F in both (*4e*) and (*2b*) sites are identical and are comparable to Sr–F bond lengths in SrF_2 (Sr–F = 2.47 Å) (Table 6).

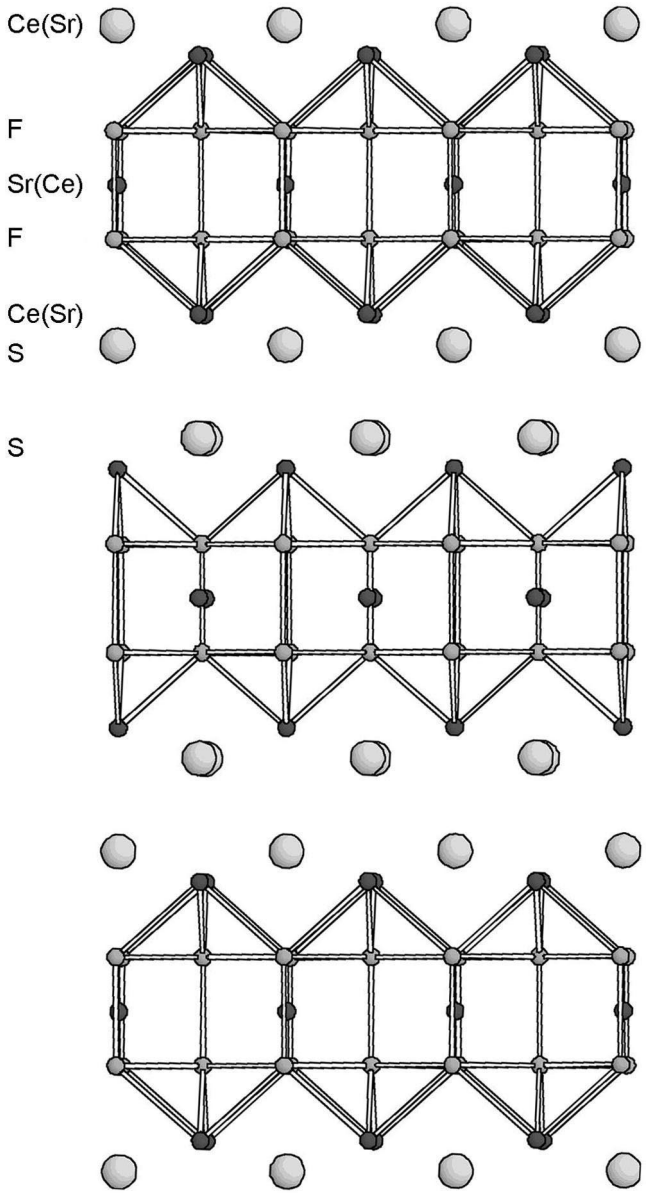

Fig. 4. Crystal structure of $Ce_2SrF_4S_2$.

Table 6
Coordination polyhedra of cerium and strontium in $Ce_2SrF_4S_2$

Distances (Å)
Ce(Sr) [*4e* site]–F: 2.43(3)×4
Ce(Sr) [*4e* site]–S(1): 2.944(4)×4
Ce(Sr) [*4e* site]–S(2): 2.99(2)×1
Sr(Ce) [*2b* site]–F: 2.44(2)×8

However these distances are shorter than the Ln–F bond lengths found in CeSF (Ce–F = 2.43 Å in $Ce_2SrF_4S_2$, Ce–F = 2.56 Å in CeSF). Thus the $[Ce_2SrF_4]^{4+}$ blocks are more compact than the $[Ce_2F_2]^{4+}$ layers in CeSF. That leads to a relaxation of Ce–S distances in $Ce_2SrF_4S_2$. As far as the Ce(Sr)–S bond distances are concerned, there are four Ce(Sr)–S distances at 2.94 Å comparable to those found in CeSF (Ce–S = 2.94 Å) and a longer one at 2.99 Å, longer than that determined in CeSF (Ce–S = 2.91 Å).

The crystal field (*5d*) created by sulphur atoms is much larger than that produced by fluorine atoms. Thus, taking into account that the fifth Ce–S bondlength along the *c* axis decreases in $Ce_2SrF_4S_2$ in comparison with that in CeSF while the four other Ce–S distances remain identical in both of these compounds, one can consider in a first approximation that the crystal field splitting [Ce(5d)] must decrease in $Ce_2SrF_4S_2$ compared to CeSF. Moreover, the increase of the fifth Ce–S bondlength in $Ce_2SrF_4S_2$ leads to a decrease of the nephelauxetic effect and in order to compensate the reduction of the Ce–S interactions, a stabilization of the *4f* levels occur.

3.2. Chromatic properties

The diffuse reflectance spectra of various fluorosulfides are represented in Fig. 5 (CeSF, SmSF, $Sm_{0.66}Gd_{0.33}SF$, $Ce_2SrF_4S_2$). The absorption edges (sulfides and fluorosulfides) corresponding to the maximum of the second derivative of the absorption curve, are reported in Table 7. In rare earth sulfides and fluorosulfides there are several bands (valence and conduction) and energy levels where electronic transitions at the origin of the color take place:

- The conduction band characterized by the 5d states of the rare earth; the splitting of the 5d band governed by the crystal field increases as the rare earth size decreases (from La to Gd).
- The valence band characterized by the 3p states of the sulfur; the bandwith increases when the Ln–S distance decreases, i.e. the covalency raises.
- The 4f levels of rare earth, where the stabilization related to the ionization energy of rare earth increases as the number of f electrons decreases.

In lanthanum sulfide and fluorosulfides, because of the absence of f electrons the most probable mechanism is

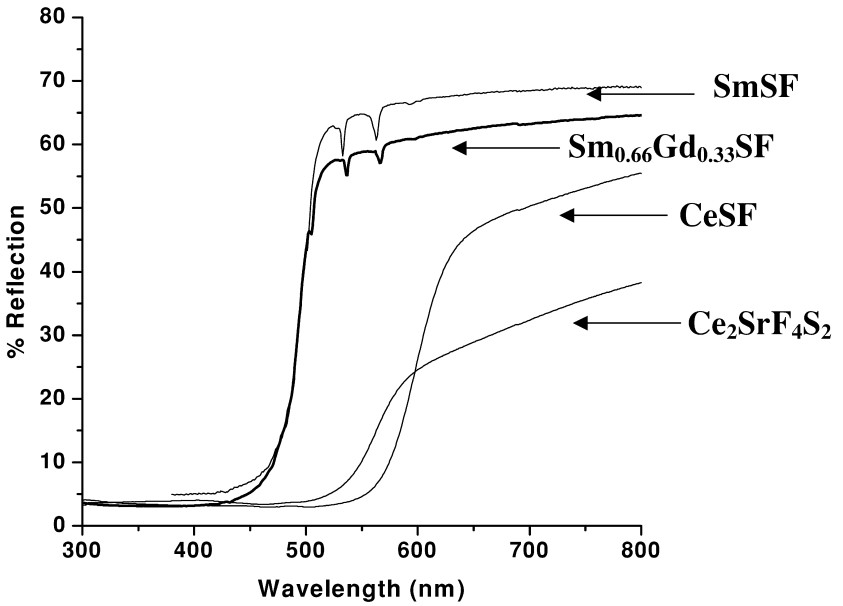

Fig. 5. Diffuse reflectance spectra of CeSF, SmSF, $Sm_{0.66}Gd_{0.33}SF$ and $Ce_2SrF_4S_2$.

3p(S)→5d(La). In cerium sulfide and fluorosulfides, the red color is probably due to electronic transitions from 4f to 5d(Ce) because of the ionization energy (4f→5d) of Ce^{3+} [12,13]. Band structure calculations of γ-Ce_2S_3 compound [2] show that the 4f level is above the 3p(S) band and the 4f→5d electronic transition is at the origin of the red color. In CeSF the same electronic transition occurs. In the case of $Ce_2SrF_4S_2$ fluorosulfides, the stabilization of the 4f level related to the increase of the fifth Ce–S bondlength, as well as the reduction of the (5d) crystal field splitting (destabilization of the 5d[t_{2g}] band) leads to an increase of the 4f→5d energy gap. Thus the 4f→5d electronic transition appears at higher energies in $Ce_2SrF_4S_2$ compared to CeSF. In the case of samarium sulfide or fluorosulfides, the transition $4f^5 \rightarrow 4f^4 5d^1$ seems impossible because of the too high value of the ionization energy 4f→5d of Sm^{3+} which tends to stabilize the 4f level. Moreover in SmSF as well as in γ-Sm_2S_3, the decrease of Sm–S distances compared to La(Ce)–S, leads to an increase of the covalency gap and the 3p(S) bandwidth. Thus a probable transition at the origin of the yellow color could be 3p(S)→4f(Sm). As far as the GdSF compound is concerned, because of the electronic configuration of $Gd^{3+}(4f^7)$ and the high value of the 4f→5d ionization energy [12,13], the same mechanism as in LaSF can be proposed: 3p(S)→5d(Gd). Moreover the absorption edges of GdSF, SmSF and $Sm_{0.66}Gd_{0.33}SF$ are similar and electronic transitions at the origin of the colour are quite different because these ions (Gd^{3+} and Sm^{3+}) have almost the same environment but different electronic configurations. Schematic band diagrams are represented in Fig. 6.

In order to explain the variation of absorption edge value as a function of the rare earth (La, Ce, Sm, Gd), ionization energies have been simply considered. The electronegativity (χ) and the hardness (η) of an element are function of ionization potential (I) and electronic affinity (A): $\chi = (I + A)/2$, $\eta = (I - A)/2$. According to Koopmans theorem, the ionization potential is simply the orbital energy of the HOMO (highest occupied molecular orbital) and the electronic affinity is the negative of the orbital energy of the LUMO (lowest unoccupied molecular orbital). Thus the hardness, $\eta = (\epsilon_{LUMO} - \epsilon_{HOMO})/2 = (I - A)/2$, is related to the energy gap [14]. Calculations of the difference between the fourth and the third ionization

Table 7
Absorption edges (nm) of LnSF and $SrLn_2S_4$ compounds

Compounds	LaSF	CeSF	SmSF	GdSF	$SrLa_2S_4$	$SrCe_2S_4$	$SrSm_2S_4$	$SrGd_2S_4$
Number of f e^-	0	1	5	7	0	1	5	7
Absorption edge (nm)	443	597	490	490	440	580	535	460
Difference of ionization energies (IV–III) (MJ/mol) for rare earths	2.97	1.594	1.74	2.25	2.97	1.594	1.74	2.25

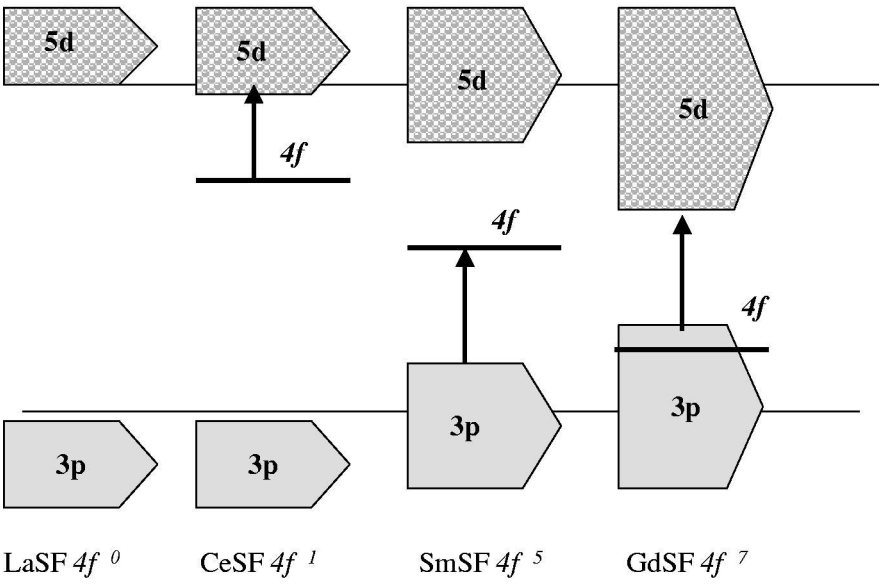

Fig. 6. Schematic band diagrams of LnSF (Ln=La, Ce, Sm, Gd).

energies of rare earth show that this value varies in a first approximation as the energy of the absorption edge (Table 7).

For $SrLn_2S_4$, the variation of the energy gap is in good agreement with the evolution of the difference of ionization energies. For rare earth fluorosulfides, the surprising results concern GdSF where the energy of the absorption edge is equal to that of SmSF, the value of the difference of ionization energies for Gd^{3+} ions being much larger than that for Sm^{3+}. This confirm that the mechanism is drastically different between SmSF and GdSF and must involve the 4f level on the curve of Sm^{3+}.

The red color of trivalent cerium sulfides and fluorosulfides is partly due to the relatively low value of the fourth ionization energy of Ce compared to the other rare earths. In $NaLaS_2$ (420 nm) and $NaGdS_2$ (360 nm) sulfides which crystallize in NaCl type structure, the absorption edges is not in good agreement with the difference of ionization energies. In these compounds where the rare earth is six-fold coordinated to sulfur the covalency is stronger than in LnSF or $SrLn_2S_4$ and the evolution of the band gap in the case of $NaGdS_2$ is due to the stabilization of 3p(S) band and the increase of the covalency.

4. Conclusion

New fluorosulfides LnSF and $Ln_2AF_4S_2$ (A=Ca, Sr) have been prepared by solid state route. The crystal structures have been determined on the basis of XRD data (powder and single crystal). In these compounds the rare earth is 4-fold coordinated to fluorine and 5-fold coordinated to sulfur, while the rare earth is 8-fold coordinated to sulfur in the sesquisulfides γ-Ln_2S_3. The Ln–F and Ln–S bond lengths decrease gradually as a function of rare earth size. In the case of $Ln_2AF_4S_2$ compounds, the Ln–F distances become smaller than those of LnSF, and the Ln–S apical distance is larger. For instance from CeSF to $Ce_2SrF_4S_2$ compounds, because of the variation of the fifth Ce–S bondlength, one can consider in a first approximation that the (5d) crystal field splitting decreases and the 4f level becomes more stabilized.

Structural features have been correlated to chromatic properties. Various electronic transitions at the origin of the color in rare earth fluorosulfides have been proposed. Most of transitions, except Ce(4f→5d), are the result of charge transfer mechanism from 3p(S) band to rare earth (4f, 5d) bands. Because the nephelauxetic and the crystal field are stronger with sulfur that fluorine, interactions between rare earth and sulfur are predominant in the mechanism of color. Rare earth-fluorine bonds participate indirectly to the mechanism by reinforcing the Ln–S interactions. One should point out that the absorption edge energies of rare earth fluorosulfides vary in a first approximation as the difference between the fourth and the third ionization energies of rare earth.

References

[1] J. Flahaut, L. Domange, M. Patrie, Bull. Soc. Chim. (1962) 2048.
[2] R. Mauricot, P. Gressier, M. Evain, R. Brec, J. Alloys Comp. 223 (1995) 130.
[3] H. Laronze, A. Demourgues, A. Tressaud, L. Lozano, J. Grannec, F. Guillen, P. Macaudière, P. Maestro, J. Alloys Comp. 275–277 (1998) 113.
[4] J. Flahaut, J. Solid. Stat. Chem. 9 (1974) 124.
[5] M.C. Dagron, F. Thevet, Ann. Chim. 6 (1971) 67.
[6] S.S. Batsanov, V.S. Filatkina, G.N. Kustova, Izv. Akad. Nauk SSSR, Ser. Khim. 6 (1971) 1190.
[7] L. Brixner, G. Hyatt, Mat. Res. Bull. 19 (1984) 745.

[8] A. Demourgues, A. Tressaud, H. Laronze, P. Macaudière, J. Fluor. Chem. 107 (2001) 215.
[9] J. Rodriguez-Carvajal, Fullprof, Vers. 3-2, LLB-CEA, Saclay, 1997.
[10] G.M. Sheldrick, SHELXL93, A Program For Refinement of Crystal Structure, University of Göttingen, Göttingen, 1993.
[11] S.G. Gurman, N. Binsted, I. Rossy, J. Phys. C 19 (1986) 1845.
[12] C.K. Jorgensen, in: Structure and Bonding, Vol. 22, Springer Verlag, 1975.
[13] J. Sugar, J. Reader, J. Chem. Phys. 59 (4) (1973) 2083.
[14] R.G. Pearson, J. Chem. Edu. 76 (2) (1999) 267.